# Paramagnetic Carbon-13 NMR Relaxation Studies on the Kinetics and Mechanism of the $HCO_3^-/CO_2$ Exchange Catalyzed by Manganese(II) Human Carbonic Anhydrase I

Jens J. Led* and Ebbe Neesgaard

*Department of Chemical Physics, University of Copenhagen, The H. C. Ørsted Institute, Universitetsparken 5, DK-2100 Copenhagen Ø, Denmark*

*Received April 3, 1986; Revised Manuscript Received September 12, 1986*

ABSTRACT: A detailed analysis of the stability and activity of Mn(II) human carbonic anhydrase I and the kinetics and mechanism of its catalysis of the $HCO_3^-/CO_2$ exchange have been performed at pH 8.5. The analysis was based on the paramagnetic relaxation rates $R_{1p}$ and $R_{2p}$ of the $^{13}C$ atom of $HCO_3^-$ in the $Mn^{2+}$/apoenzyme/$HCO_3^-/CO_2$ system and the $HCO_3^- \rightleftarrows CO_2$ interconversion rate obtained by the magnetization-transfer technique. The $R_{1p}$ and $R_{2p}$ rates were measured as functions of the temperature, magnetic field strength, and substrate and apoenzyme concentrations and were interpreted on the basis of the Solomon–Bloembergen–Morgan theories and general equations for the ligand exchange [Led, J. J., & Grant, D. M. (1977) *J. Am. Chem. Soc. 99*, 5845–5858]. From the analysis of the data, a formation constant for the Mn(II) enzyme of log $K_{MA}^{M} = 5.8 \pm 0.4$ was obtained while the activity of the Mn(II) enzyme, measured as the $HCO_3^-/CO_2$ interconversion rate at $[HCO_3^-] = 0.100$ M and pH 8.5, was found to be about 4% of that of the native Zn(II) enzyme. However, an effective dissociation constant $K_{eff}^{HCO_3^-} \lesssim 12$ mM and a maximal exchange rate constant $k_{cat}^{exch} \simeq 400\ s^{-1}$, also derived by the analysis, result in an apparent second-order rate constant $k_{cat}^{exch}/K_{eff}^{HCO_3^-}$ only a factor of 4 smaller than the corresponding rate constant for the native Zn(II) isoenzyme I. Most conspicuously, the resulting distance of only $2.71 \pm 0.03$ Å between the $Mn^{2+}$ ion of the enzyme and the $^{13}C$ atom of $HCO_3^-$ in the enzyme–bicarbonate complex indicates that the bicarbonate is bound to the metal ion by *two* of its oxygen atoms in the central catalytic step, thereby supporting the modified Zn(II)–OH mechanism [Lindskog, S., Engberg, P., Forsman, C., Ibrahim, S. A., Jonsson, B.-H., Simonsson, I., & Tibell, L. (1984) *Ann. N.Y. Acad. Sci. 429*, 61–75 (and references cited therein)]. In contrast, this binding mode differs from the structure of the complexes suggested in the rapid-equilibrium kinetic model [Pocker, Y., & Deits, T. L. (1983) *J. Am. Chem. Soc. 105*, 980–986; Pocker, Y., & Deits, T. L. (1984) *Ann. N.Y. Acad. Sci. 429*, 76–83].

The molecular mechanism by which the zinc-containing metalloenzyme carbonic anhydrase (EC 4.2.1.1) catalyzes the reversible $CO_2/HCO_3^-$ hydration/dehydration

$$CO_2 + H_2O \rightleftarrows HCO_3^- + H^+ \quad (1)$$

has been the subject of numerous investigations [Pocker and Sarkanan (1978) and references cited therein, Lindskog (1982) and references cited therein, and Bertini et al. (1982) and references cited therein]. In particular NMR and stopped-flow kinetic studies under equilibrium and steady-state conditions, respectively, have provided valuable information about the catalytic mechanism of this highly efficient enzyme. From this information, detailed, although not completely concordant, models have been derived.

Thus, Steiner et al. (1976), Simonsson et al. (1979, 1982), and Lindskog et al. (1984) (and references cited therein) have derived a kinetic scheme that essentially consists of two consecutive half-reactions:

$$E^- + CO_2 \underset{k_{-1}}{\overset{k_1}{\rightleftarrows}} E^-{\cdot}CO_2 \underset{k_{-2}}{\overset{k_2}{\rightleftarrows}} EH{\cdot}HCO_3^- \underset{k_{-3}}{\overset{k_3}{\rightleftarrows}} EH + HCO_3^- \quad (2)$$

$$EH \rightleftarrows HE \quad (3a)$$

$$HE + B \rightleftarrows E^- + BH^+ \quad (3b)$$

that is, a $CO_2/HCO_3^-$ exchange and a buffer-facilitated proton transfer between the catalytic site and the reaction medium that includes at least one intramolecular proton transfer (eq 3a). In eq 2 and 3, $E^-$ and EH are enzyme forms in which the catalytic group is deprotonated and protonated, respectively, while HE is a form in which the proton of the catalytic group has been transferred to a group in the enzyme different from the catalytic group.

Alternatively, Pocker and Deits (1982, 1983, 1984) have suggested a rapid-equilibrium kinetic model that, in some respects, is fundamentally different from the model given by eq 2 and 3. In particular, the rapid-equilibrium model, as proposed for the catalytic mechanism of bovine isoenzyme II, assumes that the C–O bond breaking in the $CO_2/HCO_3^-$ conversion and the intramolecular proton transfer (eq 3a) coincide. As pointed out by Tibell et al. (1984), this dependence of the $CO_2/HCO_3^-$ conversion on the intramolecular $H^+$ transfer step would require (1) that the maximal $CO_2/HCO_3^-$ exchange rate $k_{cat}^{exch}$ shows the same $H_2O/D_2O$ isotope effect of 3–4 as observed for the turnover rates $k_{cat}^{CO_2}$ and $k_{cat}^{HCO_3^-}$ in the case of human isoenzyme II (Steiner et al., 1975) and bovine isoenzyme II (Pocker & Bjorkquist, 1977). Here, $k_{cat}^{exch}$ measures the rate of the $CO_2/HCO_3^-$ exchange cycle at chemical equilibrium from bulk $CO_2$ through the steps in eq 2 to $HCO_3^-$ and back through the reverse reactions to bulk $CO_2$, while the steady-state kinetic parameters $k_{cat}^{CO_2}$ and $k_{cat}^{HCO_3^-}$ measure the rates of the one-way hydration or dehydration reactions (eq 2 and 3), respectively. Also, the rapid-equilibrium model would require (2) that $(k_{cat}^{exch})^{-1} = (k_{cat}^{CO_2})^{-1} +$

* Author to whom correspondence should be addressed.

0006-2960/87/0426-0183$01.50/0 

$(k_{cat}^{HCO_3^-})^{-1}$. However, both (1) and (2) are in conflict with experimental observations on human carbonic anhydrase II (Simonsson et al., 1979), the isotope effect on $k_{cat}^{exch}$ being 1 while $(k_{cat}^{exch})^{-1} < (k_{cat}^{CO_2})^{-1} + (k_{cat}^{HCO_3^-})^{-1}$. Other features of the rapid-equilibrium model are the assumptions that an $E^-\cdot CO_2\cdot HCO_3^-$ complex is kinetically significant and that there is a relatively strong but nonproductive $E^-\cdot HCO_3^-$ complex, both of which imply that $HCO_3^-$ binds to the high-pH form $E^-$ of the enzyme.

In order to proceed further toward an elucidation of the molecular basis of the carbonic anhydrase catalysis, several structural and kinetic details must be clarified. Among these are (1) the exact mode of binding of $HCO_3^-$ and $CO_2$ in the central catalytic step, (2) the possibility of other binding modes for $HCO_3^-$, including a simultaneous binding of $HCO_3^-$ and $CO_2$ to the high-pH form of the enzyme, and (3) the amount (if any) of a nonproductive $E^-\cdot HCO_3^-$ complex.

Paramagnetic $^{13}C$ NMR relaxation measurements of the substrates, interacting with carbonic anhydrase in which $Zn^{2+}$ is substituted by a paramagnetic metal ion, provide a unique method of elucidating these structural and kinetic details. As demonstrated recently in the case of the relatively complex $Mn^{2+}$/adenosine 5′-triphosphate/glycine system (Led, 1985), precise and detailed information about the structure, stability, and dynamics of the complexes involved in such a ternary system can be obtained, provided a sufficiently large and versatile set of experimental NMR relaxation data is available.

Here, similar studies were performed on the quaternary $Mn^{2+}/HCO_3^-/CO_2$/human apocarbonic anhydrase I system at pH 8.5. Recently, preliminary results indicated (Led et al., 1982b) that the Mn(II) human carbonic anhydrase I formed in this system retains about 7% of the catalytic activity of the native Zn(II) enzyme when measured as the $CO_2/HCO_3^-$ exchange rate under the experimental condition applied here. Also, an upper limit of 3.2 Å for the distance between the $Mn^{2+}$ ion of the enzyme and the $^{13}C$ nucleus of $HCO_3^-$ was established, indicating the this substrate is bound directly to the metal ion.

Besides addressing the above-mentioned questions concerning the catalytic mechanism, the study here also yields information about the specific interaction between the $Mn^{2+}$ ion and human apocarbonic anhydrase I, just as it provides a detailed analysis of the activity of the Mn(II) human carbonic anhydrase I.

## Theoretical Models

The quaternary $Mn^{2+}/HCO_3^-/CO_2$/human apocarbonic anhydrase I system contains several substrate–$Mn^{2+}$ complexes that must be considered in the analysis of the paramagnetic relaxations of the substrate carbon. Thus, according to eq 2 the two enzyme complexes, $E^-\cdot CO_2$ and $EH\cdot HCO_3^-$, must be taken into account. The formations of these complexes are given by

$$E^- + CO_2 \underset{k_{-1}}{\overset{k_1}{\rightleftharpoons}} E^-\cdot CO_2$$

$$K_{E^-\cdot CO_2}^{E^-} = \frac{[E^-\cdot CO_2]}{[E^-][CO_2]} \tag{4}$$

$$EH + HCO_3^- \underset{k_3}{\overset{k_{-3}}{\rightleftharpoons}} EH\cdot HCO_3^-$$

$$K_{EH\cdot HCO_3^-}^{EH} = \frac{[EH\cdot HCO_3^-]}{[EH][HCO_3^-]} \tag{5}$$

Here the latter complex is known to involve a paramagnetic $Mn^{2+}$–$^{13}C$ interaction, whereas the $^{13}C$ atom of the $E^-\cdot CO_2$ complex shows no paramagnetic relaxation (Led et al., 1982b). Therefore, this study shall primarily focus on the $EH\cdot HCO_3^-$ complex and its associated equilibria. Further, since the results here do not allow a separation of EH and $E^-$, only an effective formation constant

$$K_{ES}^{E} = \frac{[EH\cdot HCO_3^-]}{[E^- + EH][HCO_3^-]} = \frac{[ES]}{[E][S]} \tag{6}$$

can be determined.

Also the two consecutive nonenzymatic complexes

$$M + S \rightleftarrows MS$$

$$K_{MS}^{M} = \frac{[MS]}{[M][S]} \tag{7}$$

$$MS + S \rightleftarrows MS_2$$

$$K_{MS_2}^{MS} = \frac{[MS_2]}{[MS][S]} \tag{8}$$

must be considered, M being $Mn^{2+}$ and S being either $HCO_3^-$ or $CO_3^{2-}$.

Since the complexation of $Mn^{2+}$ with the apoenzyme is relatively weak, the enzyme formation itself is important here:

$$A + M \rightleftarrows AM(\equiv E)$$

$$K_{E}^{M} = \frac{[E]}{[A][M]} \tag{9}$$

A being the apoenzyme and E being the active metalloenzyme. Here the stability constants were expressed as $K(T) = K(T_0)\exp[-\Delta H(1/T - 1/T_0)/R]$, $T_0$ being a temperature within the experimental temperature range and $\Delta H$ being the formation enthalpy. Finally, the following mass-conversation relationships must be fulfilled:

$$[M]_0 = [M] + [M]_{complex} \tag{10}$$

$$[A]_0 = [A] + [E] \tag{11}$$

where $[M]_0$ and $[A]_0$ are the total $Mn^{2+}$ and apoenzyme concentrations, respectively, and [M], [A], $[M]_{complex}$, and [E] are the concentrations of the corresponding free and complex-bound species. Similar relations for $HCO_3^-$ and $CO_2$ were ignored here, since the concentrations of these species were practically unchanged by the complex formations due to the large surplus of $HCO_3^-$ and $CO_2$ relative to $Mn^{2+}$.

Like in other paramagnetic NMR studies, the large surplus of the observed ligands, combined with a fast exchange of these ligands between the free and metal-bound sites, assures a dilution of the immense paramagnetic effects on the relaxation rates of the metal-bound ligand nuclei. In return, only average NMR signals are observed that are affected by the relaxation rates characterizing all of the involved sites, as well as by the ligand exchange itself. Here, the former relaxation rates depend, among other things (see below), on the distance between the metal ion and the observed ligand nuclei in the metal complexes involved. Hence, the paramagnetic contribution to the experimental relaxation rates give, inter alia, information about the exchange of the ligands and their mode of binding to the metal ions.

The theoretical model for this combination of influences has been described previously for the case of exchange among three and more sites (Led & Grant, 1977; Led, 1980, 1985), and only those equations necessary for the analysis here will be shown. Thus, the paramagnetic contributions $R_{kp}$ ($k$ = 1 or 2) to the observed relaxation rates of the ligand nuclei are

determined as $R_{kp} = R_{k,obsd} - R_{kA}$, where $R_{k,obsd}$ and $R_{kA}$ are the observed relaxation rates in corresponding $Mn^{2+}$-containing and $Mn^{2+}$-free solutions, respectively, thereby eliminating contributions from relaxation mechanisms other than those due to the presence of the paramagnetic metal ions. Further, the following generalized equations relate $R_{kp}$ to the $j$ individual exchange rates $\tau_{ij}^{-1}$ ($j \neq i$) of the metal-bound ligands and to the longitudinal and transversal relaxation rates $R_{1j}$ and $R_{2j}$, of the nuclei in these ligands:

$$R_{1p} = \frac{1}{\tau_a} - \sum_{j \neq a} \frac{R_{aj}|\mathbf{R}^{aj}|}{|\mathbf{R}^{aa}|} \tag{12}$$

$$R_{2p} = \frac{1}{\tau_a} - \sum_{j \neq a} Re\frac{S_{aj}|\mathbf{S}^{aj}|}{|\mathbf{S}^{aa}|} \tag{13}$$

where the summations are over all paramagnetic sites involved. Further, $\tau_a^{-1}$ is the reciprocal lifetime of the ligand in the metal-free state and $|\mathbf{R}^{aa}|$ and $|\mathbf{R}^{aj}|$ are the determinants of the cofactor matrices of the elements $R_{aa}$ and $R_{aj}$, respectively, the matrix $\mathbf{R}$ being the sum of the relaxation rate and chemical exchange rate matrices. Analogous definitions hold for the determinants of the corresponding complex $\mathbf{S}$ cofactor matrices.

The individual ligand exchange rates $\tau_{ji}^{-1}$, are given by the Eyring equation:

$$\frac{1}{\tau_{ji}} = \frac{kT}{h} \exp\left( -\frac{\Delta H_{ji}^{\ddagger}}{RT} + \frac{\Delta S_{ji}^{\ddagger}}{R} \right) \tag{14}$$

$\Delta H_{ji}^{\ddagger}$ and $\Delta S_{ji}^{\ddagger}$ are the enthalpy and entropy of activation, respectively, while $T$ is the temperature and $R$, $k$, and $h$ are the gas constant, Boltzmann's constant, and Planck's constant, respectively. The relaxation rates $R_{1j}$ and $R_{2j}$ of the metal-bound ligands are expressed by the Solomon–Bloembergen equations (Solomon, 1955; Solomon & Bloembergen, 1956; Reuben et al., 1970):

$$R_{1j} = \frac{2}{15}\frac{S(S+1)g^2\beta^2\gamma_I^2}{r_j^6}\left[\frac{3\tau_{c,1}}{1+\omega_I^2\tau_{c,1}^2} + \frac{7\tau_{c,2}}{1+\omega_S^2\tau_{c,2}^2}\right] + \frac{2}{3}S(S+1)\left(\frac{A_j}{\hbar}\right)^2\left[\frac{\tau_{e,2}}{1+\omega_S^2\tau_{e,2}^2}\right] \tag{15}$$

and

$$R_{2j} = \frac{1}{15}\frac{S(S+1)g^2\beta^2\gamma_I^2}{r_j^6}\left[4\tau_{c,1} + \frac{3\tau_{c,1}}{1+\omega_I^2\tau_{c,1}^2} + \frac{13\tau_{c,2}}{1+\omega_S^2\tau_{c,2}^2}\right] + \frac{1}{3}S(S+1)\left(\frac{A_j}{\hbar}\right)^2\left[\tau_{e,1} + \frac{\tau_{e,2}}{1+\omega_S^2\tau_{e,2}^2}\right] \tag{16}$$

The first and second terms in both of these equations account for the dipolar and scalar interactions, respectively, between the paramagnetic metal ion and the ligand nuclei. The associated correlation rates $\tau_{c,k}^{-1}$ and $\tau_{e,k}^{-1}$ ($k = 1$ or 2), characterizing the modulation of these interactions, are given by $\tau_{c,k}^{-1} = \tau_R^{-1} + R_{ke} + \tau_{ji}^{-1}$ and $\tau_{e,k}^{-1} = R_{ke} + \tau_{ji}^{-1}$, $R_{ke}$ and $\tau_R^{-1}$ being the relaxation rates of the unpaired electrons of the metal ion and the effective isotropic reorientation rates of the metal-bound substrate, respectively, and $\tau_{ji}^{-1}$ being the ligand exchange rate (eq 14). Further, $r_j$ is the effective metal ion–nucleus distance, $A_j/\hbar$ is the corresponding scalar coupling constant, $\beta$ is the Bohr magneton, $g$, $S$, and $\omega_S$ are the $g$ factor, the spin, and the Larmor frequency of the electron, respectively, and $\gamma_I$ and $\omega_I$ are the gyromagnetic ratio and the Larmor frequency of the nucleus, respectively. Finally, $R_{1e}$ is given by (Bloembergen & Morgan, 1961; Rubinstein et al., 1971)

$$R_{1e} = \frac{\Delta^2}{25}[4S(S+1) - 3]\left[\frac{\tau_v}{1+\omega_S^2\tau_v^2} + \frac{4\tau_v}{1+4\omega_S^2\tau_v^2}\right] \tag{17}$$

Here, $\tau_v^{-1}$ is the associated correlation rate and $\Delta$ is the zero-field splitting (ZFS) parameter. The temperature dependences of $\tau_R$ and $\tau_v$ are given by the Arrhenius expression ($k$ = R or v):

$$\tau_k = \tau_k^0 \exp(E_k/RT) \tag{18}$$

$E_k$ being the activation energy. In the derivations of eq 15–17 it is assumed that the relaxation rates are small compared to the corresponding correlation rates. Therefore, eq 15–17 are strictly applicable only if this basic assumption is fulfilled.

For $Mn^{2+}$ complexes, eq 15 and 16 can be simplified. Thus, since $R_{1e} \leq R_{2e}$, it follows that $\tau_{c,1} \geq \tau_{c,2}$, while the fact that $\omega_S \simeq 2600\omega_I$ makes $\omega_S^2\tau_{c,2}^2 \gg \omega_I^2\tau_{c,1}^2$ under normal conditions. Hence, terms in $\tau_{c,2}$ can only make a significant contribution to $R_{1j}$ and $R_{2j}$ if $\omega_S^2\tau_{c,2}^2 \leq 1$. For $Mn^{2+}$ complexes, this possibility is very unlikely since all three contributions to $\tau_{c,2}^{-1}$ for such complexes are considerably smaller than $\omega_S$ even at the lowest field applied here. Therefore in eq 15 and 16, all terms in $\tau_{c,2}$ were neglected. The same reasoning can be applied to the terms in $\tau_{e,2}$ and holds even in the case of the scalar contribution to $R_{1j}$, since $(A/\hbar)^2 \ll g^2\beta^2\gamma^2/r_j^6$; that is, in the case of $Mn^{2+}$ complexes the factor before the scaler term in eq 15 is about 2 orders of magnitude smaller than that for the dipolar term, for all practical values of $A/\hbar$ and $r_j$. Therefore, also terms in $\tau_{e,2}$ including the scalar contribution to $R_{1j}$ were neglected here.

## Experimental Procedures

*Enzyme Preparation.* Human carbonic anhydrase I was purified from human erythrocytes of outdated blood by affinity chromatography, as described previously (Led et al., 1982b). The activity of the native enzyme, as monitored by esterase activity and by magnetization-transfer measurements of the $CO_2/HCO_3^-$ exchange (Led & Gesmar, 1982a), was in close agreement with the activity found by other investigators (Khalifah, 1971; Koenig, et al., 1974; Simonsson et al., 1982). The apoenzyme was prepared from the native enzyme with dipicolinic acid as the chelating agent, as described previously (Led et al., 1982b). All equipment in contact with the enzyme was washed with 2 M sulfuric acid followed by quartz-distilled water, to remove traces of $Zn^{2+}$ and other complexing metals. All contact with the inhibitory halide ions (Maren et al., 1976) and in particular $Cl^-$ was avoided. The pH of the solutions was measured on separate aliquots, with a Radiometer PHM 62 pH meter equipped with a GK 2402C combination electrode. The aliquots were discarded after the measurement. The residual activity of the final apoenzyme was <1% of that of the Zn(II) enzyme and about 6% of that of the Mn(II) enzyme, as monitored by the $HCO_3^-/CO_2$ exchange rate determined by a magnetization-transfer experiment (Led et al., 1982b).

*Chemicals.* Ultrapure $MnSO_4 \cdot 5H_2O$ was obtained from Johnson and Matthey Chemical Ltd. $NaHCO_3$ (90% $^{13}C$) was

purchased from Stohler Isotope Chemicals. The $Zn^{2+}$ content of the bicarbonate was found to be <0.2 ppm, using a Perkin-Elmer 5000 atomic absorption spectrophotometer. All other chemicals used were of analytical reagent grade. Traces of metal ions were removed from the applied tris(hydroxymethyl)aminomethane (Tris)–sulfate buffer solution by extraction with diphenylthiocarbazone (dithizone) in carbon tetrachloride.

*NMR Samples.* Individual NMR samples were prepared for each concentration of $HCO_3^-$ and apoenzyme, while using the same batches of apoenzyme, sodium bicarbonate, 50 mM Tris–sulfate buffer pH 8.5, and a 12 mM $MnSO_4$ solution in quartz-distilled water. The protein concentration of the apoenzyme stock solution was determined from the absorbance at 280 nm, with a molar absorptivity of $5.7 \times 10^4$ $cm^{-1}$ $mol^{-1}$ and a $M_r$ of 29 000. The concentrations in the individual NMR samples were determined volumetrically. Immediately after preparation, the 2-mL samples were sealed off in 8-mm (o.d.) NMR tubes 9–10 cm long to prevent loss of $CO_2$ and reduce the gas volume above the sample to a minimum. The 8-mm tubes were mounted coaxially in 10-mm NMR tubes. $D_2O$ for field-frequency lock was placed between the two tubes. No change of the samples took place during the period of the experiments, as monitored by the $R_{1p}$ and $R_{2p}$ relaxation rates. The samples were stored at 5 °C when not in use.

*NMR Experiments.* The $^{13}C$ NMR measurements at 67.89 and 22.63 MHz were made on Bruker HX 270 and WH 90 spectrometers, respectively, without broad-band proton decoupling. A total of 40 to 120 scans were accumulated per spectrum. The 5000-Hz sweep width at 22.63 MHz and the 12 200-Hz sweep width at 67.89 MHz were defined by 4K–16K data points, depending on the line width of the $H^{13}CO_3^-$ signal. The nonselective 90° pulse was 18.0 μs at 22.63 MHz and 16.5 μs at 67.89 MHz. The temperature was measured before and after each experiment, with an $[^2H_6]$acetone/$CCl_4$ thermometer (Led & Petersen, 1978) immersed in 2 mL of the applied buffer in a 10-mm NMR tube. The spin–lattice relaxation rates $R_1$ were obtained with the $T_{Rep}$–180°–$\tau$–90° pulse sequence, using corresponding samples with and without $Mn^{2+}$ for the $R_{1,obsd}$ and $R_{1A}$ determinations, respectively. The $R_1$ rates were extracted from the peak heights of 18–23 partially relaxed Fourier-transform spectra by a nonlinear three-parameter least-squares procedure (Led, 1980). The 1$\sigma$ standard deviations of the resulting $R_1$ values were ≤2% at 67.89 MHz and ≤4% at 22.63 MHz. The spin–spin relaxation rates $R_2$ were obtained from the line width of the NMR signals, with an estimated uncertainty of 5% (minimum 1.5 $s^{-1}$). Sensitivity enhancement filterings of 3–20 Hz, depending on the line width, were applied.

The $CO_2/HCO_3^-$ exchange rates were measured by complementary sets of $^{13}C$ magnetization-transfer NMR experiments (Led & Gesmar, 1982a), at 67.89 MHz. Each set contained 17 partially relaxed spectra, the delay times being in the range of 0.005–0.8 s. Each spectrum consisted of 8500 scans to assure an acceptable signal/noise ratio for the weak $^{13}CO_2$ signal. A delay of 0.6 s was applied between each scan. The selective inversion of the $HCO_3^-$ and $CO_2$ signal, respectively, was accomplished with a DANTE pulse sequence (Bodenhausen et al., 1976; Morris & Freeman, 1978) consisting of 16 consecutive pulses each 2.6 μs long and separated by 0.9 ms, while placing the carrier frequency on the signal to be inverted.

## Results and Discussion

*Variation of $H^{13}CO_3^-$ Relaxation Rates with Temperature and Field Strength.* In order to permit an analysis of the rather complex $Mn^{2+}/HCO_3^-/CO_2$/apoenzyme system, separate measurements were made on the simpler enzyme-free subsystem $Mn^{2+}/HCO_3^-/CO_2$. The field and temperature variations of $R_{1p}$ and $R_{2p}$ of the $H^{13}CO_3^-$ carbon atom in this system are shown in Figure 1. The large $R_{2p}$ relaxation rates and the smaller but significant $R_{1p}$ rates immediately indicate an interaction in solution between $Mn^{2+}$ and $HCO_3^-$ and/or $CO_3^{2-}$ in fast exchange with free $HCO_3^-$ ($[CO_3^{2-}]/[HCO_3^-] \simeq 0.018$ at pH 8.5.) Qualitatively, the temperature dependence of the $R_{2p}$ rates at both field strengths shows that the intermediate exchange condition prevails, implying that the $R_{2p}$ rates depend on the exchange rate, $\tau_{ji}^{-1}$, as well as on the relaxation rate, $R_{2j}$, of the metal-bound ligands. Further, the substantial field dependence of the $R_{2p}$ rates shows that the effective correlation rate of the dominating relaxation mechanism can be obtained from these data. Moreover, the observed increase in $R_{2p}$ ($R_{2j}$) with increasing field strength can be accomplished only if the correlation rate itself is field-dependent. Among the contributions to the effective correlation rates, only $R_{1e}$ has this quality and only if $\omega_S^2\tau_v^2 \geq 1$. Hence, information about the electron relaxation rate can be obtained from the data. In contrast to $R_{2p}$, the $R_{1p}$ rate decreases with increasing temperature and is independent of the applied field strength in the entire experimental temperature region. This shows that $\omega_I^2\tau_{c,1}^2 \ll 1$ (eq 15) and that $\tau_{c,1}$ is unaffected by the field-dependent $R_{1e}$ rate. Consequently, the $R_{1p}$ rates do not allow an independent evaluation of $\tau_{c,1}$ and the distance $r_j$ between the $Mn^{2+}$ ion and the $^{13}C$ atom of the metal-bound $HCO_3^-$ in the enzyme-free complexes.

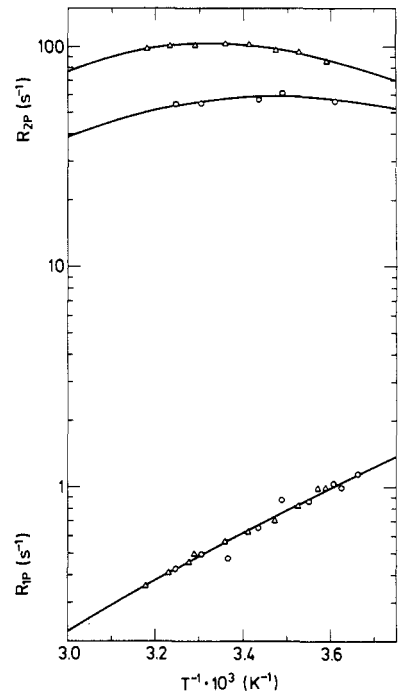


FIGURE 1: Temperature variation of the $Mn^{2+}$-induced paramagnetic contributions, $R_{1p}$ and $R_{2p}$, to the relaxation rates of the bicarbonate $^{13}C$ atom at 67.89 MHz (Δ) and 22.63 MHz (○). The sample contained $HCO_3^-$ (0.100 M) and $Mn^{2+}$ (10 μM) in Tris–sulfate buffer (50 mM) at pH 8.5. The curves correspond to the best nonlinear least-squares fit to the data in Figures 1–4.

Addition of apoenzyme to the $Mn^{2+}/HCO_3^-/CO_2$ system causes significant changes as seen in Figure 2. First, the $R_{1p}$ becomes field dependent and decreases with increasing field strength showing that $\omega_I^2\tau_{c,1}^2 \gtrsim 1$ for the enzyme-bound $HCO_3^-$. Therefore, the correlation rate $\tau_{c,1}^{-1}$, of this substrate, as well as the distance, $r_j$, between its $^{13}C$ nucleus and the $Mn^{2+}$ ion in the active site of the enzyme can be determined inde-

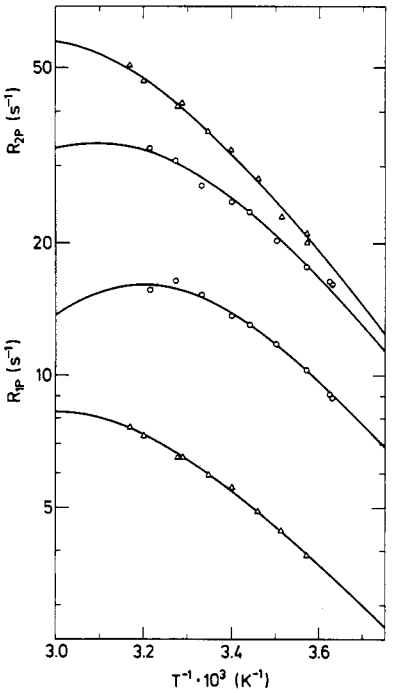


FIGURE 2: Temperature variation of the $Mn^{2+}$-induced paramagnetic contributions, $R_{1p}$ and $R_{2p}$, to the relaxation rates of the bicarbonate $^{13}C$ atom at 67.89 MHz (△) and 22.63 MHz (○). The sample contained $HCO_3^-$ (0.100 M), $Mn^{2+}$ (10 μM), and human apocarbonic anhydrase I (100 μM) in Tris–sulfate buffer (50 mM) at pH 8.5. The curves correspond to the best nonlinear least-squares fit to the data in Figures 1–4.

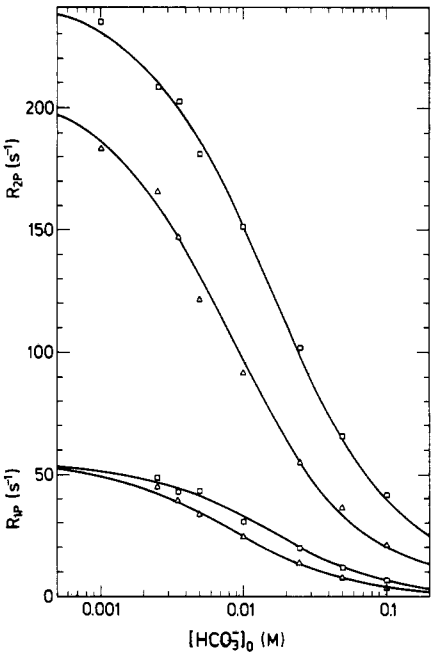


FIGURE 3: Variation with $[HCO_3^-]_0$ of the $Mn^{2+}$-induced paramagnetic contributions, $R_{1p}$ and $R_{2p}$, to the relaxation rates of the bicarbonate $^{13}C$ atom at 67.89 MHz and 280 (△) and 304 K (□). The bicarbonate concentrations were as specified, while the $Mn^{2+}$ and apoenzyme concentrations and other experimental conditions were as mentioned in Figure 2. The curves corresponds to the best nonlinear least-squares fit to the data in Figures 1–4.

pendently. Second, the slope of the $R_{2p}$ rate as a function of the temperature becomes negative, indicating a larger influence on the $R_{2p}$ rate from the exchange, $\tau_{ji}^{-1}$, of $HCO_3^-$ out of the paramagnetic site. Most surprising, however, is the simultaneous increase of $R_{1p}$ and decrease of $R_{2p}$ as compared with the enzyme-free system. Thus, $R_{1p}$ increases by a factor of 5–50, whereas $R_{2p}$ decreases by a factor of 2–5. These opposite trends immediately allow a determination of the *ratio* of substrate complexed to free and enzyme-bound $Mn^{2+}$, respectively. This, in turn, permits the *relative* values of the kinetic and structural parameters of the model to be evaluated.

*Variation of $HCO_3^-$ Relaxation Rates with Concentrations of $HCO_3^-$ and Apoenzyme.* In order to evaluate the formation constants of the involved complexes and, thereby, the *absolute* value of the kinetic and structural parameters, the $^{13}C$ relaxation rates, $R_{1p}$ and $R_{2p}$, of the bicarbonate at 67.89 MHz were measured as functions of $[HCO_3^-]$ at two temperatures as shown in Figure 3. Again, the rather different contributions to the two experimental relaxation rates from the enzyme-free and enzyme-containing complexes make these data highly informative. Similar considerations hold for the variations of the $R_{1p}$ and $R_{2p}$ rates with the apoenzyme concentration. These variations, measured at two temperatures and at two magnetic field strengths, are shown in Figure 4. A further discussion of these titration data is given in the following section.

*Quantitative Analysis of Relaxation Data.* The data were analyzed by fitting the parameters of the model described under Theoretical Models. The analysis was performed with a nonlinear least-squares procedure. The best fit was defined by the usual standard criterion (Albritton & Schmeltekopf, 1976), that is, by the minimum value of the standard deviation, $\sigma$, the individual data points being weighted with the reciprocal of their estimated uncertainties.

The simplest model that agrees with the experimental data in Figures 1–3 is basically the exchange scheme

$$\begin{array}{ccc} & & b \\ d & \underset{k_{-3}}{\overset{k_3}{\rightleftharpoons}} & a \\ & & c \end{array} \qquad (19)$$

where a is the unbound $HCO_3^-$, b and c are the enzyme-free complexes MS and $MS_2$, respectively, defined by eq 7 and 8, while d is the monocomplex between the Mn(II) enzyme and $HCO_3^-$, given by eq 6. Further, calculations show that an extension of eq 19 by an exchange reaction e ⇄ d where e is $CO_2$ in the $E^- \cdot CO_2$ complex has no effect on the $R_{1p}$ and $R_{2p}$ rates of the $HCO_3^-$ substrate for any realistic value of the exchange and relaxation rates of the carbon atom in enzyme-bound $CO_2$. Therefore, the experimental relaxation rates provide information only about the complexes in eq 19. The presence of the $MS_2$ complex is clearly revealed by the variation of the $R_{2p}$ rates with $[HCO_3^-]$. Thus, while the rest of the data in Figures 1–3 fit in with the simpler b ⇄ a ⇄ d model, the resulting parameters predict $R_{2p}$ values that increase faster with decreasing $[HCO_3^-]$ than found experimentally (Figure 3), indicating the formation of a bis-$HCO_3^-$ complex. Only a complex with a large $R_{2p}$ rate and a small $R_{1p}$ rate, like an enzyme-*free* $MS_2$ complex with relaxation rates similar to those of the MS complex, can account for this deviation without jeopardizing the agreement with the $R_{1p}$ data in Figure 3. In the calculations, the values of corresponding parameters for the MS and $MS_2$ complexes were assumed identical.

Inclusion of the apoenzyme titration data in Figure 4 provide further information about the system. First, the decrease of the $R_{1p}$ rates at the highest apoenzyme concentration shows that the correlation time $\tau_R$ depends on the concentration of the apoenzyme according to the equation (Cantor & Schimmel, 1980)

$$\tau_R = \tau_0(1 + \alpha[A]_0 + \alpha_2[A]_0^2 + \ldots) \qquad (20)$$

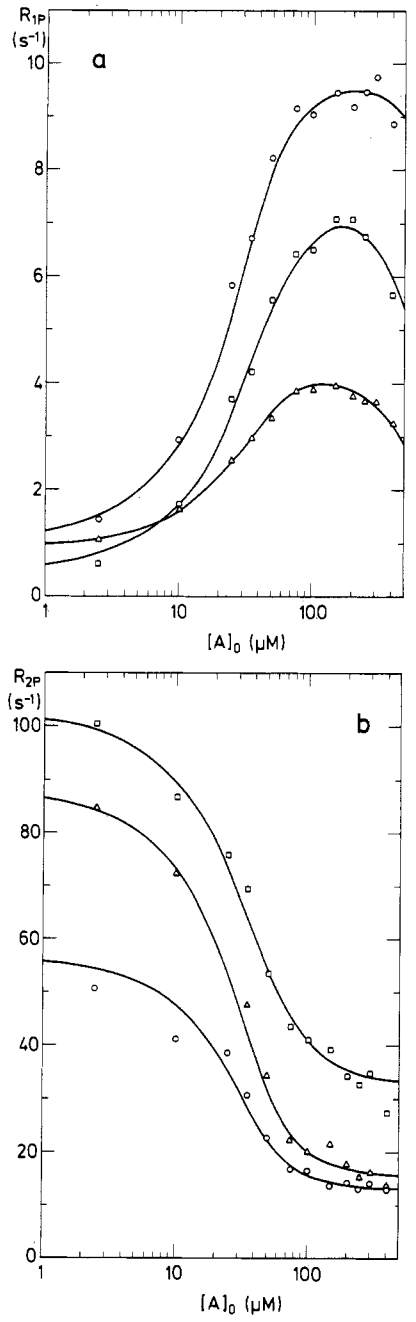


FIGURE 4: Variation with total apoenzyme concentration $[A]_0$ of the $Mn^{2+}$-induced paramagnetic contributions, $R_{1p}$ (a) and $R_{2p}$ (b), to the relaxation rates of the bicarbonate $^{13}C$ atom at 67.89 MHz and 280 (△) and 305 K (□), respectively, and at 22.63 MHz and 276 K (○). The apoenzyme concentration was as specified, while the $Mn^{2+}$ and bicarbonate concentrations and other experimental conditions were as mentioned in Figure 2. The curves correspond to the best nonlinear least-squares fit to the data in Figures 1–4.

As found in the final analysis, only the quadratic term is significant here.

Second, the dependence of both $R_{1p}$ and $R_{2p}$ on the apoenzyme concentration reveal that only a fraction of the applied apoenzyme is capable of interacting with $Mn^{2+}$ to form an active enzyme, that is

$$[A]_{active}/[A]_0 < 1 \qquad (21)$$

Indeed, when this possibility is taken into account, a simultaneous nonlinear least-squares analysis of the data in Figures 1–4 using the model in eq 6–21 results in an excellent agreement, as indicated by the full curves in Figures 1–4. The

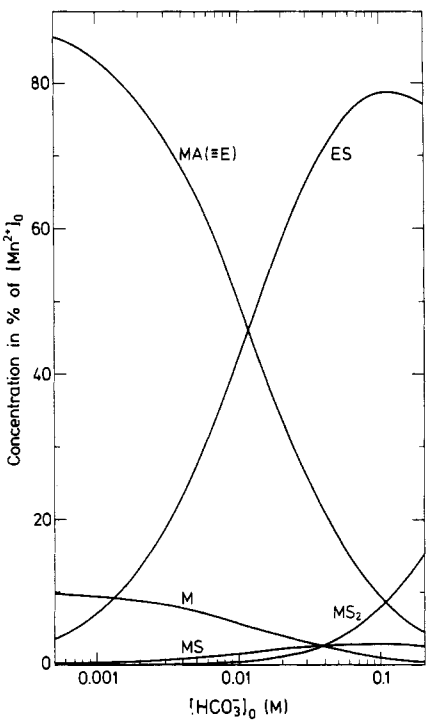


FIGURE 5: Calculated variation with $[HCO_3^-]_0$ of the composition of the $Mn^{2+}/HCO_3^-/CO_2$/human apocarbonic anhydrase I system at pH 8.5 and 298 K. The remaining experimental conditions were as specified in Figure 2. M, MS, and $MS_2$ designate the free $Mn^{2+}$ and the two consecutive complexes of $Mn^{2+}$ with $CO_3^{2-}$ or $HCO_3^-$, while MA(≡E) and ES are the free Mn(II) enzyme and the enzyme–bicarbonate complex, respectively. The curves were calculated for $[Mn^{2+}]_0 = 10$ μM, $[A]_0 = 100$ μM, $[A]_{active} = 0.23[A]_0$ (see text), and $[HCO_3^-]_0$ as specified using eq 6–11 and the stability constants in Table I.

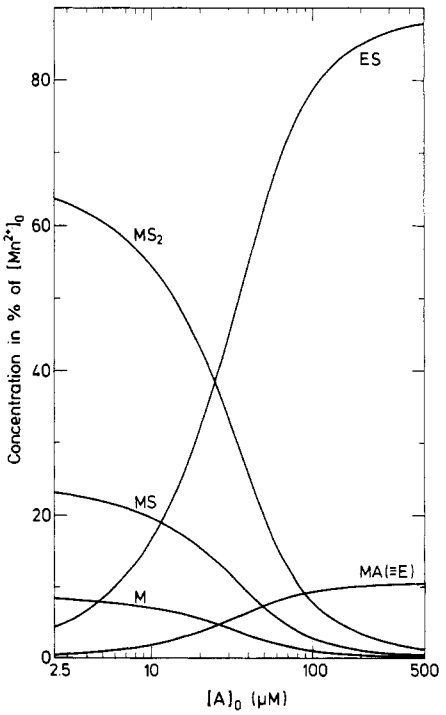


FIGURE 6: Calculated variation with total apoenzyme concentration, $[A]_0$, of the composition of the $Mn^{2+}/HCO_3^-/CO_2$/human apocarbonic anhydrase I system at pH 8.5 and 298 K. $[HCO_3^-]_0 = 0.100$ M; $[Mn^{2+}] = 10$ μM. For further specification, see the legend of Figure 5.

corresponding parameters, including the ratio $[A]_{active}/[A]_0$, are given in Table I, while the composition of the enzyme

Table I: Parameters[a] Calculated from Experimental $R_{1p}$ and $R_{2p}$ Relaxation Data of $H^{13}CO_3^-$ for Enzyme-Free $Mn^{2+}$–Carbonate/Bicarbonate Complexes MS and $MS_2$[b] (See Text) and Mn(II) Enzyme–Bicarbonate Complex ES

| | |
|---|---|
| MS and $MS_2$[b] | |
| $\Delta H^M_{MS}$ (kcal mol$^{-1}$) | −3.2 ± 1.9 |
| $K^M_{MS}$(298 K) (M$^{-1}$) | 28 ± 12 |
| $\Delta H^{\neq}_{MS}$ (kcal mol$^{-1}$) | 4.0 ± 0.5 |
| $\Delta S^{\neq}_{MS}$ (cal mol$^{-1}$ deg$^{-1}$) | −17.4 ± 1.7 |
| $\tau_{MS}^{-1}$(298 K) (s$^{-1}$) | (1.08 ± 0.14) × $10^6$ |
| $E_R$ (kcal mol$^{-1}$) | 4.0 ± 0.6 |
| $\tau_R^{-1}$(298 K) (s$^{-1}$) | (2.1 ± 0.2) × $10^{10}$ |
| $r(Mn^{2+}–^{13}C)$ (Å) | 3.00[c] |
| $E_v$ (kcal mol$^{-1}$) | 1.7 ± 0.8 |
| $\tau_v^{-1}$(298 K) (s$^{-1}$) | (4.0 ± 1.1) × $10^{10}$ |
| $\Delta G$ | 120[c] |
| $R_{1e}$(298 K, 21.1 kG) (s$^{-1}$) | (3.2 ± 0.9) × $10^6$ |
| $A_j/h$ (Hz) | (1.4 ± 0.2) × $10^5$ |
| ES | |
| $\Delta H^M_{MA}$ (kcal mol$^{-1}$) | −6 ± 4 |
| $K^M_{MA}$(298 K) (M$^{-1}$) | (6.2 ± 5.2 × $10^5$ |
| $\Delta H^E_{ES}$ (kcal mol$^{-1}$) | −4.1 ± 0.5 |
| $K^E_{ES}$(298 K) (M$^{-1}$) | 84 ± 7 |
| $\Delta H^{\neq}_{ES}$ (kcal mol$^{-1}$) | 5.2 ± 0.3 |
| $\Delta S^{\neq}_{ES}$ (cal mol$^{-1}$ deg$^{-1}$) | −16.0 ± 0.9 |
| $\tau_{ES}^{-1}$(289 K) (s$^{-1}$) | (3.01 ± 0.12) × $10^5$ |
| $E_R$ (kcal mol$^{-1}$) | 4.7 ± 0.3 |
| $\tau_R^{-1}$(298 K) (s$^{-1}$) | (1.4 ± 0.1) × $10^8$ |
| $r(Mn^{2+}–^{13}C)$ (Å) | 2.71 ± 0.03 |
| $E_v$ (kcal mol$^{-1}$) | 8 ± 5 |
| $\tau_v^{-1}$(298 K) (s$^{-1}$) | (7 ± 6) × $10^{10}$ |
| $\Delta G$ | 265[d] |
| $R_{1e}$(298 K, 21.1 kG) (s$^{-1}$) | (3 ± 2) × $10^7$ |
| $A_j/h$ (Hz) | (5.0 ± 0.4) × $10^5$ |
| $\alpha_2$ | (3.1 ± 0.2) × $10^6$ |
| $[A]_{active}/[A]_0$ | 0.23 ± 0.01 |

[a] Including 1$\sigma$ confidence limits. [b] Only average values of corresponding parameters for MS and $MS_2$ are determined; see text. [c] These parameters could not be determined from the data. Therefore, values identical with those for the $Mn^{2+}$–glycine complex (Led, 1984) were assumed. [d] Value obtained for bovine carbonic anhydrase I (Lanir et al., 1975).

system as function of the applied $HCO_3^-$ and apoenzyme concentrations, respectively, is shown in Figures 5 and 6.

The incapability of part of the apoenzyme to form the $Mn^{2+}$ derivative is most likely due to a denaturation of the protein during the preparation of the apoenzyme, considering the agreement of the activity of the applied native Zn(II) enzyme with the activity found in other studies (Khalifah, 1971; Koenig et al., 1974; Simonsson et al., 1982). Yet, irrespective of the reason for the reduced capability of the apoenzyme to interact with $Mn^{2+}$, the formation constant log $K^M_{MA}$(298 K) = 5.8 ± 0.4 obtained here for the $Mn^{2+}$–apoenzyme complex is in good agreement with a value of about 5.7 at pH 8.5, calculated for the Mn(II) bovine carbonic anhydrase II by extrapolation of the formation constants found by Lanir et al. (1975). Similarly, a slightly larger formation constant (about 6.2) is derived from the results of Wilkins and Williams (1974).

The consideration of inactive apoenzyme only affects the equilibrium constants, $K^M_{MS}$ and $K^M_{MA}$, but leaves the rest of the parameters unchanged within experimental errors, as compared with the values obtained from the data in Figures 1–3 assuming that $[A]_{active} = [A]_0$. This holds because the amount of Mn(II) enzyme being formed at the applied apoenzyme concentration (100 $\mu$M) corresponds to about 90% of the total amount of $Mn^{2+}$ (Figures 5 and 6), even for $[A]_{active} = 0.23[A]_0$ as found here. Therefore, the data in Figure 4 are not strictly necessary for the evaluation of the kinetic and structural parameters of the complexes. However, they allow an evaluation of $K^M_{MS}$ and $K^M_{MA}$, just as they improve the reliability of the conclusions and the precision of the parameters.

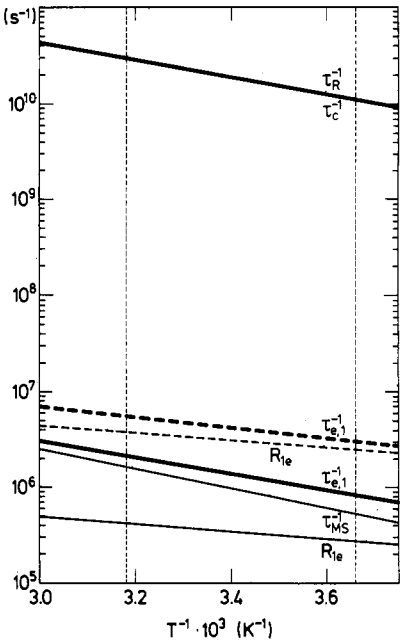


FIGURE 7: Temperature variation of correlation rates at 67.89 (—) and 22.63 MHz (– –) of the enzyme-free system specified in Figure 1. The individual correlation rates are the molecular reorientation rate, $\tau_R^{-1}$, the electron relaxation rates, $R_{1e}$, the ligand exchange rate, $\tau_{MS}^{-1}$, and the sum of these rates, $\tau_c^{-1}$ ($=\tau_R^{-1} + \tau_{MS}^{-1} + R_{1e}$) and $\tau_{e,1}^{-1}$ ($=\tau_{MS}^{-1} + R_{1e}$). The dotted, vertical lines indicate the experimental temperature region. The curves coresond to the best nonlinear least-squares fit to the data in Figures 1–4.

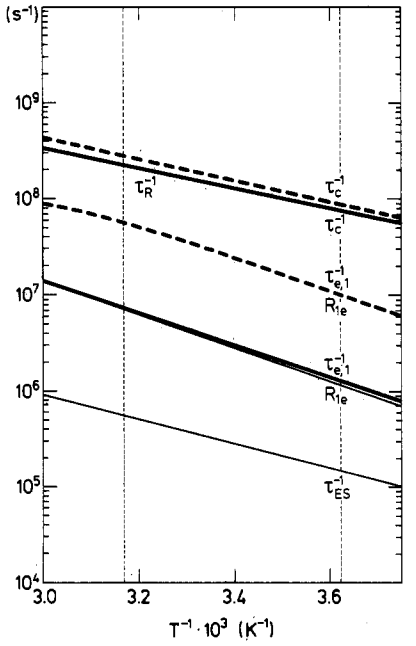


FIGURE 8: Temperature variation of correlation rates at 67.89 (—) and 22.63 MHz (– –) of the apoenzyme-containing system specified in Figure 2. For further specifications, see also Figure 7.

*Carbon-13 Relaxation of Metal-Bound $HCO_3^-$.* As revealed by the data analysis (Figure 7), the reorientation rate, $\tau_R^{-1}$, controls the correlation rate, $\tau_{c,1}^{-1}$, of the dipolar contribution to $R_{1j}$ and $R_{2j}$ in the enzyme-free complexes over the entire experimental temperature region. In contrast, the electron relaxation rate, $R_{1e}$, and the ligand exchange rate, $\tau_{MS}^{-1}$, both contribute to the effective correlation rate, $\tau_{e,1}^{-1}$, for the scalar interaction. Also in case of the enzyme–substrate complex $EH{\cdot}HCO_3^-$ the correlation rate $\tau_{c,1}^{-1}$ is dominated by $\tau_R^{-1}$, as shown in Figure 8, although there is a minor contribution from the electron relaxation, $R_{1e}$, at the low field. The $\tau_R^{-1}$ (298

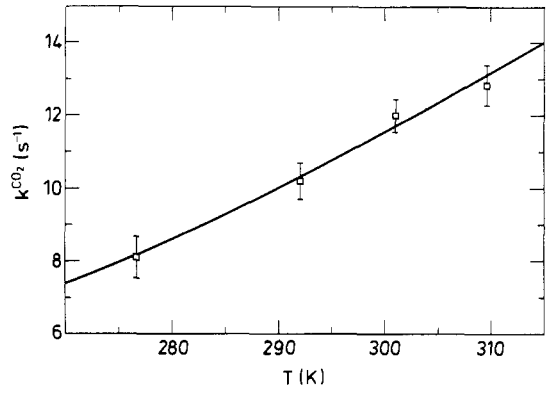


FIGURE 9: Temperature variation of $CO_2 \rightarrow HCO_3^-$ flux rate per unit $CO_2$, $k^{CO_2}$. The experimental conditions were as specified in Figure 2, and correspond to a Mn(II) enzyme concentration of 8.83 $\mu$M.

K) value obtained here (Table I) agrees closely with the value of $(1.35 \pm 0.11) \times 10^8$ $s^{-1}$ found for the corresponding bovine isoenzyme II (Navon, 1984) at the same temperature and apoenzyme concentrations, but on the basis of the relaxation of the enzyme-bound $H_2O$. The $\tau_{c,1}^{-1}$ correlation rate of the $EH{\cdot}HCO_3^-$ complex is dominated by $R_{1e}$ at both field strengths. Finally, the basic assumption, $R_{1e} \ll \tau_v^{-1}$, of the applied relaxation theory (Bloembergen & Morgan, 1961) is amply fulfilled for both the enzyme and enzyme-free complexes, as shown by the data in Table I.

A quantitative evaluation further shows that also for the dipolar dominated $R_{1j}$ rates (eq 15) is the basic assumption, $R_{1j} \ll \tau_R^{-1}$, fulfilled. As for the $R_{2j}$ rates (eq 16), the analysis reveals, first of all, that these rates are pure scalar in the enzyme-free complexes, while in the $EH{\cdot}HCO_3^-$ complex also the dipolar relaxation contributes to $R_{2j}$, ranging from 6 to 10% of $R_{2j}$ at the high field to 30–50% at low field, depending on the temperature. However, for all complexes $R_{2j} > \tau_{e,1}^{-1}$ by a factor of 5–10 at the high field although the condition $R_{2j} < \tau_{e,1}^{-1}$ still applies at the low field, $R_{2j}$ being about 10 times smaller than $\tau_{e,1}^{-1}$. Obviously, the basic assumption of the applied theory is violated for the scalar relaxation at the high field. As a consequence, the $R_{2j}$ relaxation may exceed the value predicted by the theory, approaching a solid-state value (Slichter, 1963). Primarily, this will affect the parameters $A_j/\hbar$ and $R_{1e}(\tau_v, \Delta)$ that control the $R_{2j}$ rate. In contrast, the variations of $R_{2p}$ with enzyme and substrate concentrations remain unaffected by the deviation from the model, since these variations are due entirely to changes in the amount of complexed ligands. Further, the $R_{2p}$ rate of the enzyme-bound $H^{13}CO_3^-$ at the high field is primarily controlled by the ligand exchange, as indicated by the slope of the temperature dependence (Figure 2), and depends only to a smaller extent on $R_{2j}$. Therefore, the violation of the basic assumption of the applied relaxation theory, evidenced by the inequality $R_{2j} > \tau_{e,1}^{-1}$, only gives rise to insignificant errors in the analysis.

*Estimation of Activity and $HCO_3^-/CO_2$ Exchange Kinetic Parameters.* The activity of the Mn(II) enzyme was evaluated from the $CO_2 \rightarrow HCO_3^-$ flux rate per unit $CO_2$, $k^{CO_2}$, measured by the magnetization-transfer method (Led & Gesmar, 1982a). A nonlinear least-squares analysis of the $k^{CO_2}$ rate constants at four temperatures (Figure 9), using eq 14, results in $k^{CO_2}$ (298 K) $= 11.2 \pm 0.2$ $s^{-1}$, $\Delta H^\ddagger = 1.9 \pm 0.3$ kcal $mol^{-1}$, and $\Delta S^\ddagger = -47.5 \pm 0.8$ cal $mol^{-1}$ $deg^{-1}$. Correspondingly, $k^{HCO_3^-} = k^{CO_2}[CO_2]/[HCO_3^-] = (4.26 \pm 0.08) \times 10^{-2}$ $s^{-1}$ at the applied pH of 8.5, using $pK = 6.08$ (Smith & Martell, 1976) for the acid dissociation of eq 1.

A more detailed examination of the activity was made on the basis of the relation (Simonsson et al., 1979)

$$k^{HCO_3^-} = \frac{k_{cat}^{exch}[E]_0}{K_{eff}^{HCO_3^-} + [S]} \tag{22}$$

where $k_{cat}^{exch}$ is the maximal exchange rate constant, $[E]_0$ is the total concentration of active enzyme, and [S] is the equilibrium $HCO_3^-$ concentration, while $K_{eff}^{HCO_3^-}$ is an effective dissociation constant. $K_{eff}^{HCO_3^-}$ and $k_{cat}^{exch}$ are complex functions of the individual rate and dissociation constants. For the reaction scheme given in eq 2 and 3, $k_{cat}^{exch}$ and $K_{eff}^{HCO_3^-}$ are

$$\frac{1}{k_{cat}^{exch}} = \frac{1}{k_{-1}}\left(1 + \frac{k_2}{k_{-2}}\right) + \frac{1}{k_2} + \frac{1}{k_{-2}} + \frac{1}{k_3}\left(1 + \frac{k_{-2}}{k_2}\right) \tag{23}$$

and

$$K_{eff}^{HCO_3^-} = \frac{k_3 k_2}{k_{-3}(k_2 + k_{-2})}\left(1 + \frac{K_{E1}}{[H^+]}\right) \tag{24}$$

respectively. In eqs 23 and 24 the individual rate constants refer to eq 2 while $K_{E1}$ is the dissociation constant of the catalytic group corresponding to the reaction $EH \rightarrow E^- + H^+$. Similar definitions hold for $k^{CO_2}$ and $K_{eff}^{CO_2}$.

Primarily, eq 22 allows us to correct $k^{HCO_3^-}$ for a minor contribution from residual Zn(II) enzyme. As reported previously (Led et al., 1982b), a $HCO_3^- \rightarrow CO_2$ flux rate corresponding to $k^{HCO_3^-} = (3.2 \pm 0.2) \times 10^{-2}$ $s^{-1}$ was obtained for the applied apoenzyme at pH 7.4 and $[HCO_3^-] = 0.100$ M. According to eq 22 and the kinetic parameters for the native enzyme [$k_{cat}^{exch} = (2.66 \pm 0.02) \times 10^4$ $s^{-1}$ and $K_{eff}^{HCO_3^-} \simeq$ 25 mM at pH 7.4; Simonsson et al., 1982], this rate corresponds to a residual amount of Zn(II) enzyme of about $1.1 \times 10^{-7}$ M and a $k^{HCO_3^-}$ flux rate of about $1.1 \times 10^{-2}$ $s^{-1}$ at pH 8.5 ($K_{eff}^{HCO_3^-} \simeq 280$ mM). Consequently, at pH 8.5 and $[HCO_3^-] = 0.100$ M as used here, the $HCO_3^- \rightarrow CO_2$ flux rate per unit $HCO_3^-$ catalyzed by the Mn(II) enzyme (8.83 $\mu$M) is $k^{HCO_3^-} = (4.3\text{–}1.1) \times 10^{-2} \simeq 3.2 \times 10^{-2}$ $s^{-1}$, that is, about 4% of the $k^{HCO_3^-}$ value of 0.81 $s^{-1}$, calculated for the native Zn(II) enzyme at the same pH and enzyme and substrate concentrations. The realiability of these considerations is supported by the close agreement between the $k^{HCO_3^-}$ value of $2.1 \pm 0.3$ $s^{-1}$ obtained for a 10 $\mu$M solution of Zn(II) enzyme at pH 7.5 and $[HCO_3^-] = 0.100$ M with the magnetization-transfer method (Led et al., 1982a) and the value of 2.05 $s^{-1}$ calculated from eq 22 with a $K_{eff}^{HCO_3}$ value of 30 mM at pH 7.5 (Simonsson et al., 1982).

Further details about the kinetics and activity of the applied Mn(II) isoenzyme I can be provided by combining the flux rate obtained from the magnetization-transfer experiment and the parameters derived in the analysis of the relaxation data in Figures 1–4. Thus, the $HCO_3^- \rightarrow CO_2$ flux rate $v_{exch}^{HCO_3^-}$ is given by

$$v_{exch}^{HCO_3^-} = k_{-3}[EH][HCO_3^-]\frac{k_{-2}}{k_3 + k_{-2}}\frac{k_{-1}}{k_{-1} + k_2} \tag{25}$$

where $k_{-2}/(k_3 + k_{-2})$ and $k_{-1}/(k_{-1} + k_2)$ are the probabilities of $EH{\cdot}HCO_3^-$ yielding $E^-{\cdot}CO_2$ and of $E^-{\cdot}CO_2$ yielding $CO_2$, respectively. According to a detailed balance, $k_{-3}[EH]$-$[HCO_3^-] = k_3[EH{\cdot}HCO_3^-] = \tau_{ES}^{-1}[EH{\cdot}HCO_3^-] = 2.4$ M $s^{-1}$ at 298 K (Table I and Figure 5) while $v_{exch}^{HCO_3^-} = k^{HCO_3^-}[HCO_3^-] = (3.2 \times 10^{-2}) \times 0.100 = 3.2 \times 10^{-3}$ M $s^{-1}$. Again, if one assumes that $CO_2$ is weakly bound and exchanges rapidly with the active site so that $k_2 \ll k_{-1}$, eq 25 gives a rate constant $k_{-2} \simeq 400$ $s^{-1}$ for the $EH{\cdot}HCO_3^- \rightarrow E^-{\cdot}CO_2$ conversion.

The fact, that this $k_{-2}$ value is only about 1% of the $k_{-2} \simeq k_{cat}^{HCO_3^-}$ value of $3.6 \times 10^4$ $s^{-1}$ found for the native enzyme while the $HCO_3^- \rightarrow CO_2$ flux rate is about 4% of that of the native

enzyme at the applied $[HCO_3^-]$ of 0.100 M (see above) indicates a considerably smaller effective dissociation constant, $K_{eff}^{HCO_3^-}$, for the Mn(II) enzyme. Indeed, if the previous assumption $k_{-1} \gg k_2$ is used together with the relation $k_2 \geq 10k_{-2}$ that holds since $[EH \cdot HCO_3^-]/[E^- \cdot CO_2] \geq 10$, eq 23 reduces to $k_{cat}^{exch} \simeq k_{-2}$. Subsequently, when the obtained $k_{-2}$ value of 400 $s^{-1}$ is introduced in eq 22, together with the $k^{HCO_3^-}$ value of $3.2 \times 10^{-2}$ $s^{-1}$ and the $[E]_0$ value of 8.83 $\mu$M, both corresponding to the same experimental conditions but derived from the magnetization-transfer data and the paramagnetic relaxation data, respectively, one obtains $K_{eff}^{HCO_3^-} \simeq 12$ mM, that is, an effective dissociation constant more than an order of magnitude smaller than the corresponding $K_{eff}^{HCO_3^-} \simeq 280$ mM found for the native Zn(II) enzyme at pH 8.5 (Simonsson et al., 1982).

Although the $K_{eff}^{HCO_3^-}$ value obtained here for the Mn(II) enzyme is rather uncertain due to the approximations and the experimental errors, further qualitative conclusions can be made. First, the results allow an upper limit of $K_{eff}^{HCO_3^-}$ to be established. Thus, introduction of $K_{E1}/[H^+] = [E^-]/[EH]$ into eq 24 gives $K_{eff}^{HCO_3^-} = [S][EH + E^-]/[EP + ES]$, where EP is the $E^- \cdot CO_2$ complex. By comparison $(K_{ES}^E)^{-1} = [S][EH + E^-]/[ES]$ according to eq 6. Therefore, the $(K_{ES}^E)^{-1}$ value of $12 \pm 1$ mM, obtained from the analysis of the relaxation data (Table I), is the maximum value of $K_{eff}^{HCO_3^-}$ that applies when the amount of EP is negligible. The agreement between this $(K_{ES}^E)^{-1}$ value and the value derived above for $K_{eff}^{HCO_3^-}$ suggests that the latter condition holds for the system here. However, one should notice that any significant contribution to $(k_{cat}^{exch})^{-1}$ in eq 23 from rate constants other than $k_{-2}$, would lead to a reduction of $k_{cat}^{exch}$ and to a, proportionally, even larger reduction of $K_{eff}^{HCO_3^-}$, according to eq 22.

Second, the evaluation of $k_{cat}^{exch}$ and $K_{eff}^{HCO_3^-}$ allows an estimation of the apparent second-order rate constant, $k_{cat}^{exch}/K_{eff}^{HCO_3^-}$, that applies when $[S] \ll K_{eff}^{HCO_3^-}$ (see eq 22). Thus, the conclusions above lead to the minimum value $(k_{cat}^{exch}/K_{eff}^{HCO_3^-})_{min} = 400/(12 \times 10^{-3}) = 3.3 \times 10^4$ $M^{-1}$ $s^{-1}$ at pH 8.5, that is, a value that is only 4 times smaller than the corresponding second-order rate constant of $12.5 \times 10^4$ $M^{-1}$ $s^{-1}$ obtained for the native Zn(II) enzyme at the same pH (Simonsson et al., 1982). Consequently, as the substrate concentration decreases, the $HCO_3^-/CO_2$ exchange catalyzed by the Mn(II) enzyme increases relative to the corresponding Zn(II) enzyme catalyzed rate and reaches a maximum value that is at least 25% of that of the Zn(II) enzyme, when the substrate concentration is negligible compared with the $K_{eff}^{HCO_3^-}$ value of the (Mn)II enzyme.

*Evaluation of Mechanism of $HCO_3^-/CO_2$ Interconversion.* The most conspicuous result of the data analysis is a distance of only $2.71 \pm 0.03$ Å between the $Mn^{2+}$ ion of the enzyme and the $^{13}C$ atom of $HCO_3^-$ in the enzyme–bicarbonate complex. Primarily, this distance is compatible only with a structure in which two of the $HCO_3^-$ oxygens are in close proximity to the $Mn^{2+}$ ion, indicating that both of these atoms are bound to $Mn^{2+}$ in the $EH \cdot HCO_3^-$ complex. In contrast, a $Mn^{2+}$–$^{13}C$ distance in the range of 3.0–3.2 Å should be expected if only one of the oxygen atoms was bound to $Mn^{2+}$, as found for the $Mn^{2+}$–carboxyl interactions of $Mn^{2+}$–amino acid complexes in solution (Led & Grant, 1975; Led, 1984, 1985) and in the crystal phase (Glowiak & Ciunik, 1978) or expected from the crystal structures of other metal–amino acid and metal–peptide complexes (Freeman, 1967). A relatively stable $EH \cdot HCO_3^-$ complex is further indicated by a formation constant ($K_{ES}^E = 84$ $M^{-1}$; Table I) that is more than an order of magnitude larger than the formation constants of the

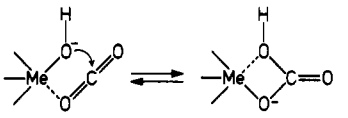

FIGURE 10: $CO_2 \rightleftarrows HCO_3^-$ interconversion step.

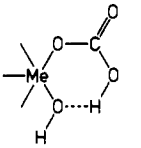

FIGURE 11: Nonproductive $E^- \cdot HCO_3^-$ complex proposed in the rapid-equilibrium model.

$Mn^{2+}$–glycine complexes formed through a $Mn^{2+}$–carboxyl interaction that only involves one oxygen atom (Led, 1984, 1985).

A central catalytic step, in which $HCO_3^-$ is attached to the metal ion (Me) by two of its oxygen atoms, is particularly interesting since it provides direct experimental evidence of the mechanism shown in Figure 10. This mechanism was proposed for the native Zn(II) enzyme by Pullman (1981) from theoretical considerations and advocated by Lindskog et al. (1983, 1984 and references cited therein) as being part of the modified zinc–hydroxide mechanism, since by this mechanism "the charged oxygen atom of $HCO_3^-$ might become coordinated to the metal ion without large movements of the atoms and without transfer of $H^+$ from the one oxygen atom of $HCO_3^-$ to another." Consequently, this mechanism makes the $CO_2/HCO_3^-$ interconversion independent of the intramolecular $H^+$ transfer (eq 3a), in agreement with the experimental observations of the Zn(II) human isoenzymes I and II (Simonsson et al., 1979, 1982). It should be noted that the mechanism proposed by Kannan et al. (1977), in which the catalytic group is Glu-106, also may involve the bidentate bicarbonate complex. However, this mechanism seems less probable since its $HCO_3^-/CO_2$ interconversion involves an intramolecular proton transfer that is likely to cause an $H_2O/D_2O$ isotope effect on $k_{cat}^{exch}$, which is not observed experimentally (Simonsson et al., 1979, 1982).

Finally, we shall examine the rapid-equilibrium kinetic model (Pocker & Deits, 1982, 1983) in light of the present results. Here the rate constant for $HCO_3^-$ leaving the enzyme after a $CO_2/HCO_3^-$ conversion is $k^{HCO_3^-}[HCO_3^-]/[EH \cdot HCO_3^-] = 3.2 \times 10^{-2} \times 0.17/7.9 \times 10^{-6} \simeq 400$ $s^{-1}$ whereas the overall rate constant, $k_3$, for $HCO_3^-$ leaving the enzyme is $3.01 \times 10^5$ $s^{-1}$. The difference between these two rate constants clearly shows that the majority of the bicarbonate–enzyme complexes are nonproductive. This agrees with the rapid-equilibrium model in that this model includes a nonproductive $E^- \cdot HCO_3^-$ complex (Figure 11) in order to account for the apparent competitive inhibition of the $CO_2$ hydration at high pH by $HCO_3^-$ (Steiner et al., 1976; Pocker & Deits, 1983). However, not only does the analysis of the relaxation data obtained here indicate the presence of only one type of ES complex at pH 8.5. More important, the short average $Mn^{2+}$–$^{13}C$ distance obtained here for the $EH \cdot HCO_3^-$ complex is incompatible with the nonproductive complex in Figure 11 as well as with any other of the complexes suggested in the rapid-equilibrium model, including the productive one, since the unidentate $Mn^{2+}$–$HCO_3^-$ interaction characterizing all of these complexes corresponds to a $Mn^{2+}$–$^{13}C$ distance in the 3.0–3.2-Å range. Hence, the structure derived here for the $EH \cdot HCO_3^-$ complex of the Mn(II) human isoenzyme I differs from the structure of the enzyme–substrate complexes proposed in the rapid-equilibrium kinetic model.

ACKNOWLEDGMENTS

We thank the Danish Natural Science Research Council for support of the Bruker HX 270 and WH 90 spectrometers. We gratefully acknowledge the free access to the RC8000 computer at the H. C. Ørsted Institute and the least-squares program FUNCFIT by G. O. Sørensen. Finally, we thank the reviewers for helpful comments.

**Registry No.** $HCO_3^-$, 71-52-3; $CO_2$, 124-38-9.

REFERENCES

Albritton, D. L., & Schmeltekopf, A. L. (1976) in *Molecular Spectroscopy: Modern Research* (Rao, K. N., & Mathews, C. W., Eds.) Vol. 2, pp 1–67, Academic, New York.

Bertini, I., Luchinat, C., & Scozzafava, A. (1982) *Struct. Bonding (Berlin) 48*, 45–92.

Bloembergen, N., & Morgan, L. O. (1961) *J. Chem. Phys. 34*, 842–850.

Bodenhausen, G., Freeman, R., & Morris, G. A. (1976) *J. Magn. Reson. 23*, 171–175.

Cantor, C. R., & Schimmel, P. R. (1980) in *Biophysical Chemistry*, Vol. 2, pp 500, 648–650, Freeman, San Francisco.

Freeman, H. C. (1967) *Adv. Protein Chem. 22*, 257–424.

Glowiak, T., & Ciunik, Z. (1978) *Acta Crystallogr., Sect. B: Struct. Crystallogr. Cryst. Chem. B34*, 1980–1983.

Kannan, K. K., Petef, M., Fridborg, K., Cid-Dresdner, H., & Lövgren, S. (1977) *FEBS Lett. 73*, 115–119.

Khalifah, R. G. (1971) *J. Biol. Chem. 246*, 2561–2573.

Koenig, S. H., Brown, R. D., London, R. E., Needham, T. E., & Matwiyoff, N. A. (1974) *Pure Appl. Chem. 40*, 103–113.

Lanir, A., Gradstajn, S., & Navon, G. (1975) *Biochemistry 14*, 242–248.

Led, J. J. (1980) *Mol. Phys. 40*, 1293–1313.

Led, J. J. (1984) *J. Chem. Phys. 88*, 5531–5537.

Led, J. J. (1985) *J. Am. Chem. Soc. 107*, 6755–6765.

Led, J. J., & Grant, D. M. (1975) *J. Am. Chem. Soc. 97*, 6962–6970.

Led, J. J., & Grant, D. M. (1977) *J. Am. Chem. Soc. 99*, 5845–5858.

Led, J. J., & Petersen, S. B. (1978) *J. Magn. Reson. 32*, 1–17.

Led, J. J., & Gesmar, H. (1982a) *J. Magn. Reson. 49*, 444–463.

Led, J. J., Neesgaard, E., & Johansen, J. T. (1982b) *FEBS Lett. 147*, 74–80.

Lindskog, S. (1982) *Adv. Inorg. Biochem. 4*, 115–170.

Lindskog, S., Ibrahim, S. A., Jonsson, B.-H., & Simonsson, I. (1983) in *The Coordination Chemistry of Metalloenzymes* (Bertini, I., Drago, R. S., & Luchinat, C., Eds.) pp 49–64, D. Reidel, Dordrecht, The Netherlands.

Lindskog, S., Engberg, P., Forsman, C., Ibrahim, S. A., Jonsson, B.-H., Simonsson, I., & Tibell, L. (1984) *Ann. N.Y. Acad. Sci. 429*, 61–75.

Morris, G. A., & Freeman, R. (1978) *J. Magn. Reson. 29*, 433–462.

Navon, G., & Kushnir, T. (1984) *Ann. N.Y. Acad. Sci. 429*, 112–113.

Pocker, Y., & Björkquist, D. W. (1977) *Biochemistry 16*, 5698–5707.

Pocker, Y., & Sarkanen, S. (1978) *Adv. Enzymol. Relat. Areas Mol. Biol. 47*, 149–274.

Pocker, Y., & Deits, T. L. (1982) *J. Am. Chem. Soc. 104*, 2424–2434.

Pocker, Y., & Deits, T. L. (1983) *J. Am. Chem. Soc. 105*, 980–986.

Pocker, Y., & Deits, T. L. (1984) *Ann. N.Y. Acad. Sci. 429*, 76–83.

Reuben, J., Reed, G. H., & Cohn, M. (1970) *J. Chem. Phys. 52*, 1617.

Rubinstein, M., Baram, A., & Luz, Z. (1971) *Mol. Phys. 20*, 67–80.

Simonsson, I., Jonsson, B.-H., & Lindskog, S. (1979) *Eur. J. Biochem. 93*, 409–417.

Simonsson, I., Jonsson, B.-H., & Lindskog, S. (1982) *Eur. J. Biochem. 129*, 165–169.

Slichter, C. P. (1963) *Principles of Magnetic Resonance*, pp 155–156, Harper and Row, New York.

Smith, R. M. & Martell, A. E. (1976) *Critical Stability Constants*, Vol. 4, p 37, Plenum, New York.

Solomon, I. (1955) *Phys. Rev. 99*, 559–565.

Solomon, I., & Bloembergen, N. J. (1956) *J. Chem. Phys. 25*, 261–266.

Steiner, H., Jonsson, B.-H., & Lindskog, S. (1975) *Eur. J. Biochem. 59*, 253–259.

Steiner, H., Jonsson, B.-H., & Lindskog, S. (1976) *FEBS Lett. 62*, 16–20.

Tibell, L., Forsman, C., Simonsson, I., & Lindskog, S. (1984) *Biochim. Biophys. Acta 789*, 302–310.

Wilkins, R. G., & Williams, K. R. (1974) *J. Am. Chem. Soc. 96*, 2241–2245.